Nonlinear feedback control of axisymmetric aerial vehicles

Daniele Pucci, Tarek Hamel, Pascal Morin, Claude Samson

Nonlinear Feedback Control of Axisymmetric Aerial Vehicles ⋆

Daniele Pucci [a], Tarek Hamel [b], Pascal Morin [c], Claude Samson [d]

[a] *Istituto Italiano di Tecnologia, Genova, Italy*

[b] *I3S/UNSA, Sophia-Antipolis, France*

[c] *Institut des Systèmes Intelligents et de Robotique, Université Pierre et Marie Curie, CNRS UMR 7222, France*

[d] *INRIA, I3S/UNSA, Sophia Antipolis, France*

Abstract

We investigate the use of simple aerodynamic models for the feedback control of underactuated aerial vehicles flying with large flight envelopes. Thrust-propelled vehicles with a body shape symmetric with respect to the thrust axis are considered. Upon a condition on the aerodynamic characteristics of the vehicle, we show that the equilibrium orientation can be explicitly determined as a function of the desired flight velocity. This allows for the adaptation of previously proposed control design approaches based on the thrust direction control paradigm. Simulation results conducted by using measured aerodynamic characteristics of quasi-axisymmetric bodies illustrate the soundness of the proposed approach.

Key words: aerodynamic forces, aircraft control, axisymmetric body, flight control, stabilizing feedback

1 Introduction

Flight control techniques have been developed primarily for full-size commercial airplanes, designed to fly along very specific trajectories (trim trajectories with a very narrow range of angles of attack). Control design is then typically achieved from the linearized equations of motion along desired trajectories. However, some aerial vehicles are required to fly in conditions that involve large and rapid variations of the angle of attack. Examples are given by fighter aircraft, convertible aircraft, or small Unmanned Aerial vehicles (UAVs) operating in windy environments. In fact, some Vertical Take-Off and Landing (VTOL) vehicles, like e.g. ducted fans, are subjected to large variations of the angle of attack when transitioning from hover to horizontal flight. It then matters to ensure large stability domains that are achievable via the use of nonlinear feedback designs. Nonlinear feedback control of aircraft can be traced back to the early eighties. Following [1], control laws based on the dynamic inversion technique have been proposed to extend the flight envelope of military aircraft (see, e.g., [2] and the references therein). The control design relies on tabulated models of aerodynamic forces and moments, like the High-Incidence Research Model (HIRM) [3]. Compared to linear techniques, this type of approach yields extended flight domains without involving gain scheduling strategies. The angle of attack is still assumed to remain in a limited range, however, away from the stall zone. Nonlinear feedback control of VTOL vehicles has been addressed with a larger variety of techniques, like dynamic inversion [4], Lyapunov-based design [5], backstepping [6], sliding modes [6,7], or predictive control [8] (See e.g. [9] for more references). Since most of these studies address the stabilization of hover flight or low-velocity trajectories, aerodynamic effects are typically ignored, or modeled as a simple additive perturbation. In highly dynamic flight or harsh wind conditions, however, aerodynamic effects become important. This raises several questions such as, e.g., *which aerodynamic models should be considered for the control design?* and *which feedback control solutions can be inferred from these models to ensure large stability domains and robustness?*

Methods used in aerodynamics to precisely describe aerodynamic forces, e.g. computational fluid dynamics or wind tunnel measurements, do not provide analytical expressions of aerodynamic characteristics (AC). From

⋆ Corresponding author: P. Morin. This work was supported by the "Chaire d'excellence en Robotique RTE-UPMC" and by the French ANR Project SCAR.

Email addresses: daniele.pucci@iit.it (Daniele Pucci), thamel@i3s.unice.fr (Tarek Hamel), morin@isir.upmc.fr (Pascal Morin), csamson@i3s.unice.fr (Claude Samson).

a control viewpoint they are useful to finely tune a controller around a given flight velocity, but exploiting them in the case of large flight envelopes (i.e., that involve strong variations of either the flight velocity or the angle of attack) is difficult. In this paper we advocate the use of simple analytical models of AC that can account for important structural properties of the system in a large flight envelope. The idea is then to exploit these properties at the control design level and rely on the robustness of feedback controllers to cope with discrepancies between the model and the true AC. More precisely, for (heavier than air) underactuated vehicles with a body-shape symmetric with respect to (w.r.t.) the thrust axis, we provide conditions on the AC under which the vehicle's equilibrium orientation associated with a desired flight velocity is explicitly (and uniquely) defined. We also show that such conditions are satisfied by simple models that approximate at the first order AC of real systems reported in the literature. The control design then essentially consists in aligning the thrust direction with the desired equilibrium orientation and monitoring the thrust intensity to compensate for the intensity of external forces. This *thrust direction control paradigm* has been exploited for underactuated VTOL vehicles either by neglecting aerodynamic effects [10], or by considering systems submitted to drag forces only [11]. Determination of the vehicle's equilibrium orientation is straightforward in these cases but it is a major issue for more general vehicles [12]. This paper shows that the thrust direction control paradigm can be extended to aerial vehicles submitted to significant lift forces.

The paper is organized as follows. Section 2 provides the notation and background. In Section 3, we show that for a class of symmetric bodies the dynamical equations of motion can be transformed into a simpler form. This transformation is used in Section 4 to propose a control design method applicable to several vehicles of interest.

2 Notation and background

$\boldsymbol{E}^3$ denotes the $3D$ Euclidean vector space and vectors in $\boldsymbol{E}^3$ are denoted with bold letters. Inner and cross products in $\boldsymbol{E}^3$ are denoted by the symbols $\cdot$ and $\times$ respectively. $\mathcal{I} = \{O; \boldsymbol{i}_0, \boldsymbol{j}_0, \boldsymbol{k}_0\}$ denotes a fixed inertial frame w.r.t. which the vehicle's absolute pose is measured (see Figure 1). This frame is chosen as the NED frame (North-East-Down). $\mathcal{B} = \{G; \boldsymbol{i}, \boldsymbol{j}, \boldsymbol{k}\}$ denotes a frame attached to the body, with $\boldsymbol{G}$ the body's center of mass. The linear and angular velocities $\boldsymbol{v}$ and $\boldsymbol{\omega}$ of the body frame $\mathcal{B}$ are then defined by

$$\boldsymbol{v} := \frac{d}{dt}\boldsymbol{OG}\,, \qquad \frac{d}{dt}(\boldsymbol{i}, \boldsymbol{j}, \boldsymbol{k}) := \boldsymbol{\omega} \times (\boldsymbol{i}, \boldsymbol{j}, \boldsymbol{k})\,, \tag{1}$$

Throughout the paper, the time-derivative is taken w.r.t. the inertial frame $\mathcal{I}$ and, for any couple of points $\boldsymbol{A}, \boldsymbol{B}$, $\boldsymbol{AB} \in \boldsymbol{E}^3$ denotes the vector from $\boldsymbol{A}$ to $\boldsymbol{B}$.

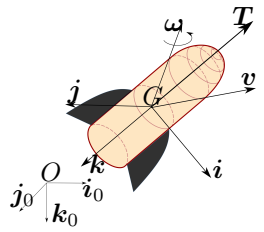

Figure 1. Notation.

2.1 Equations of motion

Aircraft are modeled as rigid bodies of constant mass controlled via four control inputs: the thrust intensity $T \in \mathbb{R}$ of a body-fixed thrust force $\boldsymbol{T} = -T\boldsymbol{k}$ and the three components of a control torque vector $\boldsymbol{\Gamma}_G$. This class of systems covers a large variety of vehicles like multi-copters, helicopters, convertibles UAVs, or even conventional airplanes. The vehicle's equations of motion are given by

$$m\dot{\boldsymbol{v}} = m\boldsymbol{g} + \boldsymbol{F}_a - T\boldsymbol{k}, \tag{2a}$$

$$\frac{d}{dt}(\boldsymbol{i}, \boldsymbol{j}, \boldsymbol{k}) = \boldsymbol{\omega} \times (\boldsymbol{i}, \boldsymbol{j}, \boldsymbol{k}), \tag{2b}$$

$$\frac{d}{dt}(\boldsymbol{J}\,\boldsymbol{\omega}) = \boldsymbol{GP} \times \boldsymbol{F}_a + \boldsymbol{\Gamma}_G. \tag{3}$$

with m the vehicle's mass, $\boldsymbol{g} = g\boldsymbol{k}_0$ the gravitational acceleration vector, $(\boldsymbol{F}_a, \boldsymbol{P})$ the resultant of the aerodynamic forces and its point of application, $\boldsymbol{G}$ the vehicle's center of mass, and $\boldsymbol{J}$ the inertia operator at $\boldsymbol{G}$. Here we implicitly assume that so-called *gyroscopic torques* and *body-forces* are negligible or that they have already been compensated for via a preliminary torque control action (See, e.g., [13], [14], [15, Ch. 3] for more details).

2.2 Aerodynamic forces

The modelling of aerodynamic forces and torques $\boldsymbol{F}_a$ and $\boldsymbol{M}_a := \boldsymbol{GP} \times \boldsymbol{F}_a$ acting on the vehicle is of particular importance, see, e.g. [16] [17, Ch. 2] for fixed-wing aircraft, [18] [14] for quadrotors, [19] [20] [15, Ch. 3] for ducted-fan tail-sitters, and [21] for helicopters. Denote by $\boldsymbol{v}_a$ the *air velocity*, i.e. $\boldsymbol{v}_a = \boldsymbol{v} - \boldsymbol{v}_w$ with $\boldsymbol{v}_w$ the wind's velocity. The aerodynamic force is typically decomposed as $\boldsymbol{F}_a = \boldsymbol{F}_L + \boldsymbol{F}_D$ where the *lift force* $\boldsymbol{F}_L$ is the component perpendicular to $\boldsymbol{v}_a$, and the *drag force* $\boldsymbol{F}_D$ is the component along $\boldsymbol{v}_a$'s direction. Consider any pair of angles (α, β) characterizing the orientation of $\boldsymbol{v}_a$ with respect to the body frame (e.g. Figure 2). Knowing that the intensity of the *steady* aerodynamic force varies approximately like $|\boldsymbol{v}_a|^2$, there exist two dimensionless positive functions C_L and C_D depending on the *Reynolds number* R_e, the *Mach number* M, and (α, β), and such that

$$\begin{aligned} \boldsymbol{F}_L &= k_a |\boldsymbol{v}_a| C_L(R_e, M, \alpha, \beta) \boldsymbol{r}(\alpha, \beta, |\boldsymbol{v}_a|) \times \boldsymbol{v}_a, \\ \boldsymbol{F}_D &= -k_a |\boldsymbol{v}_a| C_D(R_e, M, \alpha, \beta) \boldsymbol{v}_a, \\ \boldsymbol{r} \cdot \boldsymbol{v}_a &= 0, \quad |\boldsymbol{r}| = 1, \quad k_a := \rho\Sigma/2, \end{aligned} \tag{4}$$

with ρ the air density, Σ an area germane to the body shape, $\boldsymbol{r}(\cdot)$ a unit vector-valued function. C_D and C_L are the *aerodynamic characteristics* of the body, i.e. the so-called *drag* and *lift* coefficients. Here we neglect the effects of the vehicle's *rotational and unsteady motions* on its surrounding airflow (see [17, p. 199] for more details).

2.3 Reduced control model

To develop control principles that apply to many aerial vehicles, one must get free of actuation specificities. In agreement with a large number of works on VTOL control and in view of Eq. (3), which points out how $\boldsymbol{\omega}$ can be modified via the choice of the control torque $\boldsymbol{\Gamma}_G$, one can consider $\boldsymbol{\omega}$ as an intermediate control input (see [11] for details). The corresponding physical assumption is that "almost" any desired angular velocity can be obtained after a short transient time. The control model then reduces to Eqs. (2) with T and $\boldsymbol{\omega}$ as control inputs.

3 Symmetric bodies and spherical equivalence

From Eq. (2), for the body to move with a constant velocity the controlled thrust vector $T\boldsymbol{k}$ must be equal to the resultant external force $\boldsymbol{F}_{ext} := m\boldsymbol{g} + \boldsymbol{F}_a$. When $\boldsymbol{F}_a$ does not depend on the vehicle's orientation, as in the case of *spherical bodies*, $\boldsymbol{F}_{ext}$ does not depend on this orientation either. The thrust direction at the equilibrium is then unique and it is explicitly given by the direction of $\boldsymbol{F}_{ext}$. The control strategy then basically consists in aligning the thrust direction $\boldsymbol{k}$ with the direction of $\boldsymbol{F}_{ext}$ (using $\boldsymbol{\omega}$ as control input) and in opposing the thrust magnitude to the intensity of $\boldsymbol{F}_{ext}$ (using T as control input). This is the basic principle of the thrust direction control paradigm [10,11]. For most aerial vehicles, however, aerodynamic forces depend on the vehicle's orientation, and thus on the direction of $\boldsymbol{k}$. The equilibrium relation $T\boldsymbol{k} = \boldsymbol{F}_{ext}$ then becomes an implicit equation with both sides of this equality depending on $\boldsymbol{k}$. In this case, existence, uniqueness, and explicit determination of the equilibrium thrust direction(s) become fundamental questions for the control design [12]. In this section, we provide answers to these questions for a class of axisymmetric vehicles. More precisely, let us consider vehicles whose external surface $\mathcal{S}$ is characterized by the existence of an orthonormal body frame $\mathcal{B}_c = \{G_c; \boldsymbol{i}, \boldsymbol{j}, \boldsymbol{k}\}$ that satisfies either one of the following assumptions:

Assumption 1 (Symmetry) *Any point $P \in \mathcal{S}$ transformed by the rotation of an angle θ about the axis $G_c\boldsymbol{k}$, i.e. by the operator defined by $g_\theta(\cdot) = \mathrm{rot}_{G_c\boldsymbol{k}}(\theta)(\cdot)$, also belongs to $\mathcal{S}$, i.e. $g_\theta(P) \in \mathcal{S}$.*

Assumption 2 (Bisymmetry) *Any point $P \in \mathcal{S}$ transformed by the composition of two rotations of angles θ and π about the axes $G_c\boldsymbol{k}$ and $G_c\boldsymbol{j}$, i.e. by the operator defined by $\bar{g}_\theta(\cdot) = (\mathrm{rot}_{G_c\boldsymbol{k}}(\theta) \circ \mathrm{rot}_{G_c\boldsymbol{j}}(\pi))(\cdot)$, also belongs to $\mathcal{S}$, i.e. $\bar{g}_\theta(P) \in \mathcal{S}$.*

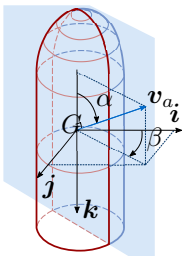

Figure 2. The (α, β) angles.

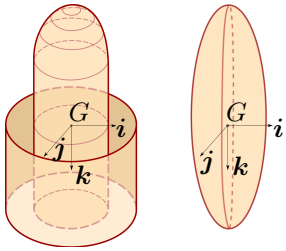

Figure 3. Symmetric and bisymmetric shapes

Here, $\mathrm{rot}_{O\boldsymbol{v}}(\psi)(P)$ denotes the rotation about the axis $O\boldsymbol{v}$ by the angle ψ of the point P. Examples of "symmetric" and "bisymmetric" shapes satisfying these assumptions are represented in Figure 3 (with $G = G_c$). Various human-made aerial devices (rockets, missiles, airplanes with annular wings, etc.) satisfy Assumption 1 in the first approximation. When this assumption holds true, one can define $\alpha \in [0, \pi]$ as the *angle of attack* between $-\boldsymbol{k}$ and $\boldsymbol{v}_a$, and $\beta \in (-\pi, \pi]$ as the angle between $\boldsymbol{i}$ and the projection of $\boldsymbol{v}_a$ on the plane $\{G_c; \boldsymbol{i}, \boldsymbol{j}\}$ (see Figure 2). Assumption 1 also implies the following properties: **P1** : the aerodynamic force $\boldsymbol{F}_a$ does not change when the body rotates about its axis of symmetry $G_c\boldsymbol{k}$; **P2** : $\boldsymbol{F}_a \in \mathrm{span}\{\boldsymbol{k}, \boldsymbol{v}_a\}$. Property P1) in turn implies that the AC do not depend on β, whereas Property P2) implies that: *i*) the unit vector $\boldsymbol{r}$ in (4) is orthogonal to $\boldsymbol{k}$ and independent of α and, *ii*) the lift coefficient is equal to zero when $\alpha = \{0, \pi\}$. Then, from Eq. (4),

$$\begin{aligned} \boldsymbol{F}_L &= k_a|\boldsymbol{v}_a|C_L(R_e, M, \alpha)\boldsymbol{r}(\beta) \times \boldsymbol{v}_a, \\ \boldsymbol{F}_D &= -k_a|\boldsymbol{v}_a|C_D(R_e, M, \alpha)\boldsymbol{v}_a, \\ \boldsymbol{r}(\beta) &= -\sin(\beta)\boldsymbol{i} + \cos(\beta)\boldsymbol{j}. \end{aligned} \tag{5}$$

The above choice of (α, β) also yields:

$$\boldsymbol{v}_a = |\boldsymbol{v}_a|(\sin(\alpha)\cos(\beta)\boldsymbol{i} + \sin(\alpha)\sin(\beta)\boldsymbol{j} - \cos(\alpha)\boldsymbol{k})$$

so that, from (5)

$$\begin{aligned} &\boldsymbol{r}(\beta) \times \boldsymbol{v}_a = -\cot(\alpha)\boldsymbol{v}_a - \tfrac{|\boldsymbol{v}_a|}{\sin(\alpha)}\boldsymbol{k}, \\ &\boldsymbol{F}_a = -k_a|\boldsymbol{v}_a|\Big[\Big(C_D(\cdot) + C_L(\cdot)\cot(\alpha)\Big)\boldsymbol{v}_a + \tfrac{C_L(\cdot)}{\sin(\alpha)}|\boldsymbol{v}_a|\boldsymbol{k}\Big]. \end{aligned} \tag{6}$$

For constant Reynolds and Mach numbers the AC depend only on α and the following result follows from (6).

Proposition 1 *Consider an axisymmetric thrust-propelled vehicle subjected to aerodynamic forces given by* (5)*. Assume that*

$$C_D(\alpha) + C_L(\alpha)\cot(\alpha) = C_{D_0}, \tag{7}$$

with C_{D_0} constant. Then, Eq. (2) *can be written as*

$$m\dot{\boldsymbol{v}} = m\boldsymbol{g} + \boldsymbol{F}_p - T_p\boldsymbol{k}, \tag{8}$$

with

$$T_p = T + k_a|\boldsymbol{v}_a|^2 \frac{C_L(\alpha)}{\sin(\alpha)},\ \boldsymbol{F}_p(\boldsymbol{v}_a) = -k_a C_{D_0}|\boldsymbol{v}_a|\boldsymbol{v}_a. \quad (9)$$

This proposition is the core result of this paper. It shows that an axisymmetric body subjected to both drag and lift forces can be seen as a sphere subjected to the orientation independent drag force $\boldsymbol{F}_p$ and powered by the thrust force $\boldsymbol{T}_p = -T_p\boldsymbol{k}$. As shown further on, it then becomes possible to rely on existing techniques to design feedback stabilizers. In particular, it follows from (8) that given a desired reference velocity $\boldsymbol{v}_r$, there exists a unique (up to sign) equilibrium thrust direction $\boldsymbol{k}_{ref}$ as long as $|m\boldsymbol{g} + \boldsymbol{F}_p - m\dot{\boldsymbol{v}}_r| \neq 0$ along this reference velocity. More precisely,

$$\boldsymbol{k}_{ref} = \frac{m\boldsymbol{g} + \boldsymbol{F}_p(\boldsymbol{v}_{r,a}) - m\dot{\boldsymbol{v}}_r}{|m\boldsymbol{g} + \boldsymbol{F}_p(\boldsymbol{v}_{r,a}) - m\dot{\boldsymbol{v}}_r|}$$

where $\boldsymbol{v}_{r,a} = \boldsymbol{v}_r - \boldsymbol{v}_w$. This holds true provided that the AC satisfy (7). An example of simple functions C_L, C_D that satisfy (7) and the π-periodicity property w.r.t. α associated with *bisymmetric* bodies is given next.

Proposition 2 *The functions C_D and C_L defined by*

$$C_D(\alpha) = c_0 + 2c_1\sin^2(\alpha),\ C_L(\alpha) = c_1\sin(2\alpha), \quad (10)$$

with c_0 and c_1 two real numbers, satisfy Condition (7) with $C_{D_0} = c_0 + 2c_1$. Eq. (9) then yields:

$$T_p = T + 2c_1k_a|\boldsymbol{v}_a|^2\cos(\alpha),\ \boldsymbol{F}_p(\boldsymbol{v}_a) = -k_aC_{D_0}|\boldsymbol{v}_a|\boldsymbol{v}_a.$$

The proof is straightforward.
A particular bisymmetric body is the sphere whose AC (zero lift coefficient and constant drag coefficient) are obtained by setting $c_1 = 0$ in (10). Elliptic-shaped bodies are also bisymmetric but in contrast with the sphere they do generate lift. Approximation of measured AC with functions given by (10) is illustrated by the Figure 4 (left) with experimental data borrowed from [22, p.19] for an elliptic-shaped body ($R_e = 7.96 \cdot 10^6$, $M = 6$). The identified coefficients are $c_0 = 0.43$ and $c_1 = 0.462$. Since missile-like devices are "almost" bisymmetric, approximating their AC with such functions can also be attempted. For instance, the approximation shown in Figure 4 (right) uses experimental data taken from [23, p.54] for a missile moving at $M = 0.7$. In this case, $c_0 = 0.1$ and $c_1 = 11.55$. In both cases the approximation should be good enough for feedback control purposes.

4 Control design

The results of Section 3 are now exploited for the control design of axisymmetric vehicles. We start by revisiting the thrust direction control problem.

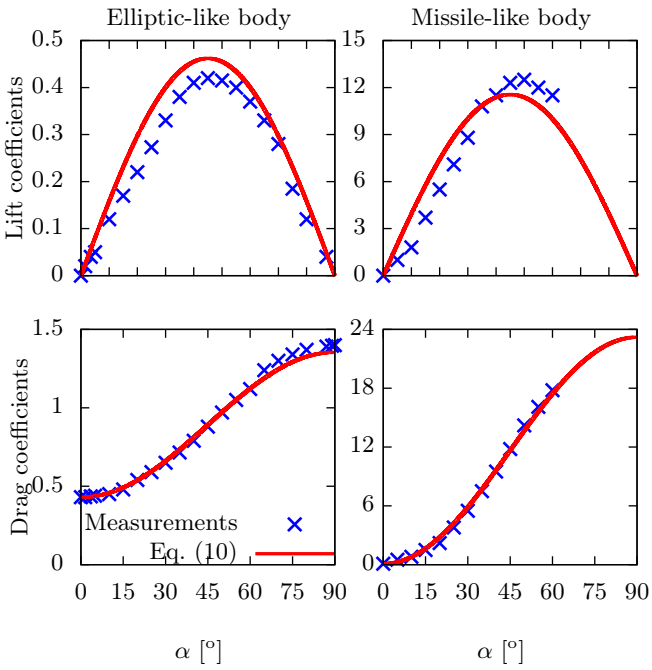

Figure 4. AC of elliptic and missile-like bodies.

4.1 Thrust direction control

Consider a time-varying reference thrust (unitary) direction $\boldsymbol{k}_r$. It is assumed that $\boldsymbol{k}_r$ varies smoothly with time so that $\dot{\boldsymbol{k}}_r(t)$ is well defined for all t. The following result provides control expressions for the angular velocity control input $\boldsymbol{\omega}$ yielding a large stability domain.

Proposition 3 *The feedback law*

$$\boldsymbol{\omega} = \left(k_1(\boldsymbol{k},t) + \frac{\dot{\gamma}(t)}{\gamma(t)}\right)\boldsymbol{k}\times\boldsymbol{k}_r + \boldsymbol{\omega}_r + \lambda(\boldsymbol{k},t)\boldsymbol{k} \quad (11)$$

with $\boldsymbol{\omega}_r = \boldsymbol{k}_r \times \dot{\boldsymbol{k}}_r$ the instantaneous angular velocity of $\boldsymbol{k}_r$, $\lambda(\cdot)$ any real-valued continuous function, $\gamma(\cdot)$ any smooth positive real-valued function such that $\inf_t \gamma(t) > 0$, and $k_1(\cdot)$ any continuous positive real-valued function such that $\inf_{\boldsymbol{k},t} k_1(\boldsymbol{k},t) > 0$, ensures exponential stability of the equilibrium $\boldsymbol{k} = \boldsymbol{k}_r$ with domain of attraction $\{\boldsymbol{k}(0) : \boldsymbol{k}(0)\cdot\boldsymbol{k}_r(0) \neq -1\}$.

The proof is given in the appendix.
The above expression of $\boldsymbol{\omega}$ is a coordinate-free generalization of the solution proposed in [11], for which the control gain γ was not present and a specific choice of k_1 was imposed. The first term in the right-hand side of (11) is a feedback term depending on the error between $\boldsymbol{k}$ and $\boldsymbol{k}_r$. The second term is a feedforward term. The last term is associated with the rotation about the axis $\boldsymbol{k}$. It does not affect the thrust direction dynamics since $\dot{\boldsymbol{k}} = \boldsymbol{\omega}\times\boldsymbol{k}$. Let us comment on the choice of the control

gains. Concerning $\lambda(\cdot)$, the simplest choice is $\lambda(t) \equiv 0$. Another possibility is $\lambda(t) = -\boldsymbol{\omega}_r(t) \cdot \boldsymbol{k}(t)$. This yields $\boldsymbol{\omega}(t) \cdot \boldsymbol{k}(t) = 0$ so that the control does not induce instantaneous rotation about $\boldsymbol{k}$. Concerning γ and k_1, constant gains can be chosen but other choices can be preferred. For instance, $k_1(\boldsymbol{k}, t) = k_{1,0}/(1 + \boldsymbol{k} \cdot \boldsymbol{k}_r(t) + \epsilon_1)$, with $k_{1,0} > 0$ and ϵ_1 a small positive number, grows large when $\boldsymbol{k}$ gets close to $-\boldsymbol{k}_r$, thus making this undesired equilibrium more repulsive.

4.2 Velocity and position control

Let $\boldsymbol{v}_r(\cdot)$ denote a reference velocity time-function (at least three times differentiable everywhere). Velocity control consists in the asymptotic stabilization of the velocity error $\tilde{\boldsymbol{v}} := \boldsymbol{v} - \boldsymbol{v}_r$ at zero. This control objective may be complemented by the convergence to zero of a position error $\tilde{\boldsymbol{p}} := \boldsymbol{p} - \boldsymbol{p}_r$, with $\boldsymbol{p}_r(\cdot)$ a reference position time-function. In this case, $\boldsymbol{v}_r = \dot{\boldsymbol{p}}_r$, and the error state vector to be stabilized at zero contains the six-dimensional vector $(\tilde{\boldsymbol{p}}, \tilde{\boldsymbol{v}})$. The error vector may further include an integral of the position error $\tilde{\boldsymbol{p}}$. In order to address various control problems, we consider a "generalized" control objective consisting in the asymptotic stabilization at zero of an error vector denoted as $(\tilde{\boldsymbol{\rho}}, \tilde{\boldsymbol{v}})$, with $\tilde{\boldsymbol{\rho}} \in \mathbb{R}^p$ and such that $\dot{\tilde{\boldsymbol{\rho}}} = \boldsymbol{f}(\tilde{\boldsymbol{\rho}}, \tilde{\boldsymbol{v}})$, with $\boldsymbol{f}(\cdot, \cdot)$ denoting a smooth vector-valued function. For instance, if $\tilde{\boldsymbol{\rho}} = \tilde{\boldsymbol{p}}$ with $\tilde{\boldsymbol{p}}$ denoting either a position error or an integral of the velocity error $\tilde{\boldsymbol{v}}$, then $\boldsymbol{f}(\tilde{\boldsymbol{\rho}}, \tilde{\boldsymbol{v}}) = \tilde{\boldsymbol{v}}$. If $\tilde{\boldsymbol{\rho}} = (\boldsymbol{I}_p, \tilde{\boldsymbol{p}})$, with $\boldsymbol{I}_p$ denoting a saturated integral of the position tracking error such that $\frac{d}{dt}\boldsymbol{I}_p = h(\tilde{\boldsymbol{\rho}})$, then $\boldsymbol{f}(\tilde{\boldsymbol{\rho}}, \tilde{\boldsymbol{v}}) = (h(\tilde{\boldsymbol{\rho}}), \tilde{\boldsymbol{v}})$. The simplest case is pure velocity control without integral correction, i.e. $\tilde{\boldsymbol{\rho}} = \emptyset$. Consider now an axisymmetric vehicle. From (8),

$$\begin{aligned} m\dot{\tilde{\boldsymbol{v}}} &= \boldsymbol{F}_p + m(\boldsymbol{g} - \boldsymbol{a}_r) - T_p\boldsymbol{k} \\ &= m\boldsymbol{\xi} + \bar{\boldsymbol{F}}_p - T_p\boldsymbol{k}, \end{aligned} \tag{12}$$

with $\boldsymbol{a}_r := \dot{\boldsymbol{v}}_r$ the reference acceleration and

$$\bar{\boldsymbol{F}}_p(\boldsymbol{v}_a, \boldsymbol{a}_r, \boldsymbol{\xi}) := \boldsymbol{F}_p(\boldsymbol{v}_a) + m(\boldsymbol{g} - \boldsymbol{a}_r - \boldsymbol{\xi}). \tag{13}$$

The idea is to end up working with the simple control system $\dot{\tilde{\boldsymbol{v}}} = \boldsymbol{\xi}$ where $\boldsymbol{\xi}$ plays the role of a virtual feedback term. To this aim Eq. (12) suggests to make $\bar{\boldsymbol{F}}_p - T_p\boldsymbol{k}$ converge to zero. With T_p preferred positive, this implies that the thrust direction $\boldsymbol{k}$ should tend to

$$\boldsymbol{k}_r := \bar{\boldsymbol{F}}_p/|\bar{\boldsymbol{F}}_p| \ . \tag{14}$$

Recall from (9) that $\boldsymbol{F}_p$ does not depend on $\boldsymbol{k}$. Thus, provided that $\boldsymbol{\xi}$ does not depend on $\boldsymbol{k}$, $\bar{\boldsymbol{F}}_p$ does not depend on $\boldsymbol{k}$ either, and $\boldsymbol{k}_r$ is well defined as long as $\bar{\boldsymbol{F}}_p$ does not vanish. This is precisely what makes Proposition 1 important for the control design. Convergence of $\bar{\boldsymbol{F}}_p - T_p\boldsymbol{k}$ to zero also implies that T_p must tend to $\bar{\boldsymbol{F}}_p \cdot \boldsymbol{k}$. From (2) and (8), this is equivalent to the convergence of the thrust intensity T to $\bar{\boldsymbol{F}}_a \cdot \boldsymbol{k}$ with

$$\bar{\boldsymbol{F}}_a := \boldsymbol{F}_a + m(\boldsymbol{g} - \boldsymbol{a}_r - \boldsymbol{\xi}) \tag{15}$$

Once the reference thrust direction $\boldsymbol{k}_r$ is well defined, a stabilizing feedback law can be designed:

Proposition 4 *Consider an axisymmetric vehicle with aerodynamic characteristics satisfying relation* (7)*, and a smooth feedback controller $\boldsymbol{\xi}(\tilde{\boldsymbol{\rho}}, \tilde{\boldsymbol{v}})$ for the control system*

$$\dot{\tilde{\boldsymbol{\rho}}} = \boldsymbol{f}(\tilde{\boldsymbol{\rho}}, \tilde{\boldsymbol{v}}) \tag{16a}$$

$$\dot{\tilde{\boldsymbol{v}}} = \boldsymbol{\xi} \tag{16b}$$

Assume that

A1 : *$\boldsymbol{\xi}(\tilde{\boldsymbol{\rho}}, \tilde{\boldsymbol{v}})$ makes $(\tilde{\boldsymbol{\rho}}, \tilde{\boldsymbol{v}}) = (\boldsymbol{0}, \boldsymbol{0})$ a locally exponentially stable equilibrium point of System* (16)*;*

A2 : *$\bar{\boldsymbol{F}}_p$ does not vanish along the velocity reference trajectory $\boldsymbol{v}_r$, i.e., $\exists \delta > 0 \ : \ \delta \leq |\bar{\boldsymbol{F}}_p(\boldsymbol{v}_{r,a}(t), \boldsymbol{a}_r(t), \boldsymbol{0})|$, $\forall t$, with $\boldsymbol{v}_{r,a} := \boldsymbol{v}_r - \boldsymbol{v}_w$.*

Then, $T = \bar{\boldsymbol{F}}_a \cdot \boldsymbol{k}$ and $\boldsymbol{\omega}$ given by (11)*, with $\boldsymbol{k}_r$ defined by* (14)*, $\gamma = \sqrt{c_2 + |\bar{\boldsymbol{F}}_p|^2}$, and c_2 any strictly positive constant, ensure local exponential stability of the equilibrium point $(\tilde{\boldsymbol{\rho}}, \boldsymbol{v}, \boldsymbol{k}) = (\boldsymbol{0}, \boldsymbol{v}_r, \boldsymbol{k}_r)$ for the system* (16a)-(2)*.*

The proof is given in the appendix. Let us comment on the above result.

1) Proposition 4 shows how to derive an exponential stabilizer for the underactuated System (2) from an exponential stabilizer for the fully-actuated system $\dot{\tilde{\boldsymbol{v}}} = \boldsymbol{\xi}$, e.g., a linear feedback controller.

2) Given an exponential stabilizer $\boldsymbol{\xi}$ for System (16), local exponential stability of zero tracking errors for an axisymmetric vehicle for which the AC satisfy relation (7) relies on Assumption A2, which imposes that the *reference* thrust direction $\boldsymbol{k}_{ref}$, i.e. along the reference trajectory, is well defined at all times. This condition may be violated for very specific and aggressive reference trajectories. Note, however, that its satisfaction can be checked from the knowledge of the reference velocity only (provided that an accurate model of AC is available).

3) Feedback control calculation calls for a few remarks. A difficulty is that both $\boldsymbol{k}_r$ and γ depend on $\bar{\boldsymbol{F}}_p$. Since $\dot{\gamma}$ and $\dot{\boldsymbol{k}}_r$ are involved in the calculation of $\boldsymbol{\omega}$, the time-derivative of $\bar{\boldsymbol{F}}_p$ has to be calculated also. In this respect, in view of (8) and the way T_p is calculated, note that $\dot{v}$ and subsequently $\dot{\bar{\boldsymbol{F}}}_p$ do not depend on ω. This guarantees the well-posedness of the control calculation provided only that $\boldsymbol{k}_r$ is well defined. In practice, it is also possible to estimate $\dot{\bar{\boldsymbol{F}}}_p$ using the calculation of $\bar{\boldsymbol{F}}_p$ and a high-gain observer. Another possibility is to use the reference velocity instead of the vehicle's actual velocity to calculate an approximation of this term.

Proposition 4 guarantees *local* asymptotic stability only. The difficulty to ensure a large domain of convergence comes from the risk of $\bar{\boldsymbol{F}}_p$ vanishing at some point, which would in turn make $\boldsymbol{k}_r$, as specified by (14), ill-defined. This risk, although small, cannot be ruled out, especially because the term $\boldsymbol{F}_p$ in $\bar{\boldsymbol{F}}_p$ can be very large due to aerodynamic forces. In practice, having a control always well defined requires to modify the term $\bar{\boldsymbol{F}}_p$ used in the control expression so that it cannot vanish. This is a subject of future studies. Assuming that $\bar{\boldsymbol{F}}_p$ remains different from zero, then convergence of the tracking errors can be guaranteed, as specified by the following proposition the proof of which follows from that of Proposition 4.

Proposition 5 *Consider the feedback law of Proposition 4. Assume further that $\boldsymbol{\xi}(\tilde{\boldsymbol{\rho}}, \tilde{\boldsymbol{v}})$ globally asymptotically stabilizes the origin $(\tilde{\boldsymbol{\rho}}, \tilde{\boldsymbol{v}}) = (\boldsymbol{0}, \boldsymbol{0})$ of the system*

$$\begin{aligned} \dot{\tilde{\boldsymbol{\rho}}} &= \boldsymbol{f}(\tilde{\boldsymbol{\rho}}, \tilde{\boldsymbol{v}}) \\ \dot{\tilde{\boldsymbol{v}}} &= \boldsymbol{\xi}(\tilde{\boldsymbol{\rho}}, \tilde{\boldsymbol{v}}) + \varepsilon(t) \end{aligned} \tag{17}$$

when $\varepsilon(\cdot)$ is identically zero, and still ensures the convergence to zero of the solutions to this system when $\varepsilon(\cdot)$ converges to zero exponentially. Then, any solution to the closed-loop system (16a)-(2) *along which $\bar{\boldsymbol{F}}_p$ does not vanish (in the sense that $\exists \delta > 0 \ : \ \delta \leq |\bar{\boldsymbol{F}}_p(\boldsymbol{v}_a(t), \boldsymbol{a}_r(t), \boldsymbol{\xi}(\tilde{\boldsymbol{\rho}}, \tilde{\boldsymbol{v}}))|, \ \forall t$) converges to the equilibrium point $(\boldsymbol{0}, \boldsymbol{v}_r, \boldsymbol{k}_r)$.*

4.3 Simulation results

We consider a missile-like body with AC given by the measurements of Figure 4 (right). The control objective is the asymptotic stabilization at zero of the velocity error $\tilde{\boldsymbol{v}}$. A saturated integral $\tilde{\boldsymbol{\rho}} = \boldsymbol{I}_v$ of this error is used in the control law in order to compensate for static modelling errors and additive perturbations. $\boldsymbol{I}_v$ is obtained as the (numerical) solution to the following equation [24]:

$$\dot{\boldsymbol{I}}_v = \boldsymbol{f}(\tilde{\boldsymbol{\rho}}, \tilde{\boldsymbol{v}}) = -k_I \boldsymbol{I}_v + k_I \mathrm{sat}^{\delta}\left(\boldsymbol{I}_v + \frac{\tilde{\boldsymbol{v}}}{k_I}\right) \ ; \ \boldsymbol{I}_v(0) = 0,$$

with k_I a positive gain, $\delta > 0$ the upperbound of $|\boldsymbol{I}_v|$, and sat^{δ} a differentiable approximation of the classical saturation function defined by $\mathrm{sat}^{\delta}(\boldsymbol{x}) = \min\left(1, \frac{\delta}{|\boldsymbol{x}|}\right)\boldsymbol{x}$. The feedback law of Proposition 4 is applied with $\boldsymbol{\xi}(\tilde{\boldsymbol{\rho}}, \tilde{\boldsymbol{v}}) = -k_v \tilde{\boldsymbol{v}} - k_i \boldsymbol{I}_v$, $k_1(\boldsymbol{k}, t) = k_{1,0}/(1 + \boldsymbol{k} \cdot \boldsymbol{k}_r(t) + \epsilon_1)^2$, and $\lambda(\boldsymbol{k}, t) = -\boldsymbol{\omega}_r(t) \cdot \boldsymbol{k}(t)$, where $k_v = 5, k_i = k_v^2/4, k_I = 50$, $k_{1,0} = 10$, and $\epsilon_1 = 0.01$. The feedforward term $\boldsymbol{\omega}_r$ is evaluated using the reference acceleration $\dot{\boldsymbol{v}}_r$ rather than the vehicle's acceleration $\dot{\boldsymbol{v}}$ calculated from Newton's equation (2) and the model of aerodynamic forces $\boldsymbol{F}_a$. The simulated vehicle's equations of motion are given by (2)-(5), with the AC C_L and C_D obtained by interpolating the measurements reported in [23, p.54] (see Figure 4 (right)). These coefficients thus differ from the approximating functions (10) used in the control calculation, here computed by using the identified coefficients $c_0 = 0.1$ and $c_1 = 11.55$ reported previously. The missile's physical parameters are $m = 100\,[Kg]$ and $(\rho, \Sigma) = (1.292, 0.5)$ $(\left[Kg/m^3\right], [m]^2)$, so that $k_a \approx 0.3\ [Kg/m]$. These values are replaced by estimated ones, namely $\hat{k}_a = 0.24$ and $\hat{m} = 80\ [Kg]$, in the control calculation in order to test the control robustness w.r.t. parametric uncertainties. In particular, the vector $\bar{\boldsymbol{F}}_p$ in (13) is calculated with $\boldsymbol{F}_p(\boldsymbol{v}_a) = -\hat{k}_a(c_0 + 2c_1)|\boldsymbol{v}_a|\boldsymbol{v}_a$. The reference velocity expressed in Mach numbers is:

$$\boldsymbol{v}_r(t) = \begin{cases} 0.7\boldsymbol{i}_0 & 0 \leq t < 10, \\ -0.7\boldsymbol{j}_0 & 10 \leq t < 20, \\ -0.7\boldsymbol{k}_0 & 20 \leq t < 30, \\ -0.7\boldsymbol{i}_0 & 30 \leq t < 40, \end{cases} \tag{18}$$

and $\boldsymbol{v}_r(t) = -0.5\sin(t\pi/5)\boldsymbol{i}_0 + 0.6\sin(t\pi/10)\boldsymbol{j}_0 + 0.6\cos(t\pi/10)\boldsymbol{k}_0$ when $40 \leq t < 60$. The applied thrust force and angular velocity $\boldsymbol{\omega} = (\boldsymbol{i}, \boldsymbol{j}, \boldsymbol{k})\omega$ are saturated as follows: $0 < T < 10\hat{m}g$, $|\omega_i| < 2\pi$, $\quad i = \{1, 2, 3\}$. The initial velocity and attitude are: $\boldsymbol{v}(0) = 0.5\boldsymbol{i}_0\ \ [Mach]$, $\phi_0 = \psi_0 = 0°$, $\theta_0 = -40°$ where (ϕ, θ, ψ) denote standard *roll*, *pitch*, and *yaw* angles as defined in [17, p. 47].

From top to bottom, Figure 5 shows the evolution of the reference velocity $\boldsymbol{v}_r = (\boldsymbol{i}_0, \boldsymbol{j}_0, \boldsymbol{k}_0)\dot{x}_r$, the vehicle's velocity $\boldsymbol{v} = (\boldsymbol{i}_0, \boldsymbol{j}_0, \boldsymbol{k}_0)\dot{x}$, the angle of attack α, the angular velocity $\boldsymbol{\omega} = (\boldsymbol{\imath}, \boldsymbol{\jmath}, \boldsymbol{k})\omega$, the applied thrust-to-weight ratio, the norm of $\bar{\boldsymbol{F}}_p$ (which must be different from zero to ensure the well-posedness of the control solution), and the angle $\tilde{\theta}$ between $\boldsymbol{k}$ and $\boldsymbol{k}_r$. There is no wind. The initial angle of attack at $t = 0$ is 50°. The attitude control makes this angle decrease rapidly. Sharp discontinuities of $\dot{x}_r$ at $t = 10, 20, 30, 40$ are responsible for the observable transitions and temporarily large angles of attack. Thanks to the integral correction terms, $\dot{x}$ converges to $\dot{x}_r$ when $\dot{x}_r$ is constant. For $40 \leq t < 60$, although $\dot{x}_r$ varies rapidly velocity errors remain small, thanks to both feedforward and integral correction terms. Figure 6 illustrates the improvement brought by the control proposed in this paper w.r.t. a control that does not take the dependence of the aerodynamic forces upon the vehicle's orientation into account. To this aim, we consider the velocity control proposed in [11] for spherical-like vehicles subjected to aerodynamic drag solely. This control is basically the same as the one considered in Proposition 4 with $\bar{\boldsymbol{F}}_a$ used in place of $\bar{\boldsymbol{F}}_p$ in the control law. Figure 6 shows the evolution of $|\bar{\boldsymbol{F}}_a|$ and $\tilde{\theta}$ when applying this control, with the feedforward term $\boldsymbol{\omega}_r$ (whose calculation involves $\dot{\boldsymbol{F}}_a$) set equal to zero for the sake of simplification. One can observe from this figure that i) relative variations of the norm of $|\bar{\boldsymbol{F}}_a|$ are significantly more pronounced than those of $|\bar{\boldsymbol{F}}_p|$ in Figure 5, ii) the amplitude of the orientation error $\tilde{\theta}$ after a discontinuous change of the reference velocity is much more important, and even more significantly iii) $\bar{\boldsymbol{F}}_a$ crosses zero little after the reference velocity discontinuity occurring

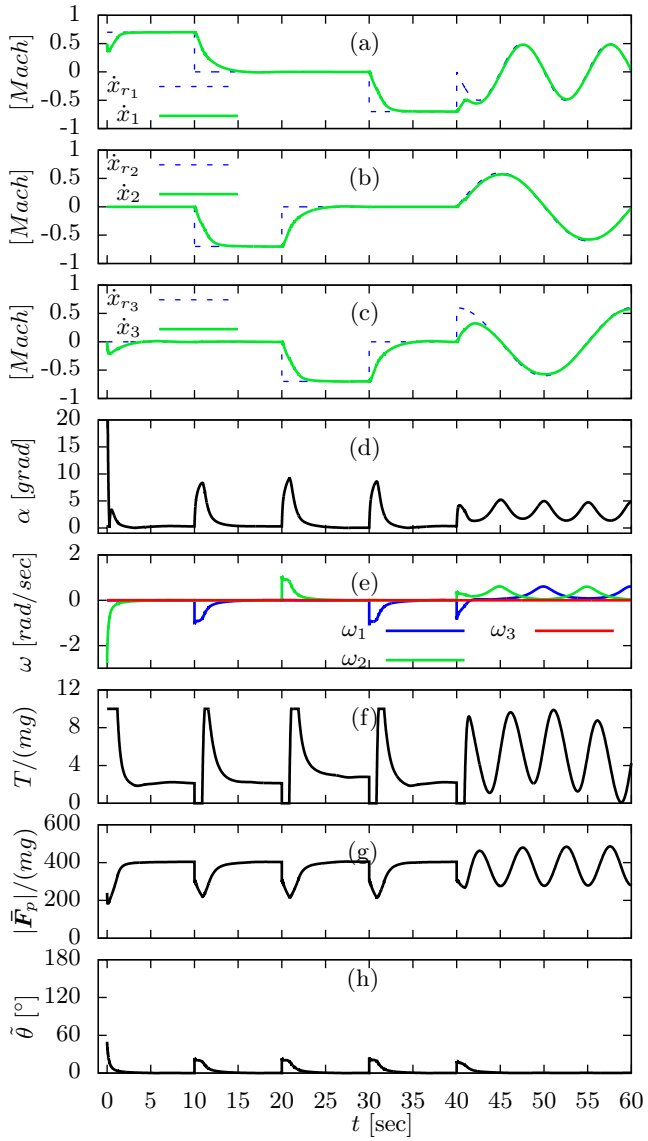

Figure 5. C-701 simulation with $\bar{\boldsymbol{F}}_p$ in angular control.

at $t = 40$. The reference direction $\boldsymbol{k}_r$ and thus the control law, are not defined at this point, thus leading to an abrupt stop of the simulation.

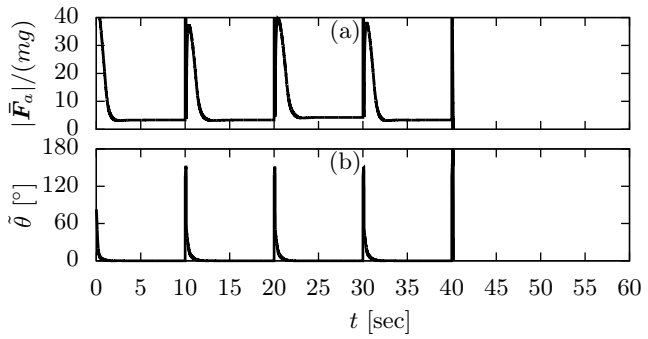

Figure 6. C-701 simulation with $\bar{\boldsymbol{F}}_a$ in angular control.

5 Conclusion and perspectives

Extension of the thrust direction control paradigm to a class of vehicles with axisymmetric body shapes has been addressed. Application examples include, e.g., rockets and aerial vehicles with annular wings. Specific aerodynamic properties associated with these particular shapes allow for the design of nonlinear feedback controllers yielding asymptotic stability in a very large flight envelope. Simulation results for bisymmetric and quasi-bisymmetric bodies validate the proposed control approach. Further extension of the present approach to vehicles with non-symmetric body shapes (e.g. conventional airplanes) is currently investigated.

Appendix

We make use of the following classical vectorial relations:

$$\begin{aligned} &\forall \boldsymbol{x},\boldsymbol{y},\boldsymbol{z} \in \boldsymbol{E}^3,\ \ \boldsymbol{x}\cdot(\boldsymbol{y}\times\boldsymbol{z}) = \boldsymbol{y}\cdot(\boldsymbol{z}\times\boldsymbol{x}) \\ &\forall \boldsymbol{x},\boldsymbol{y},\boldsymbol{z} \in \boldsymbol{E}^3,\ \ \boldsymbol{x}\times(\boldsymbol{y}\times\boldsymbol{z}) = (\boldsymbol{x}\cdot\boldsymbol{z})\boldsymbol{y} - (\boldsymbol{x}\cdot\boldsymbol{y})\boldsymbol{z} \end{aligned} \tag{19}$$

Proof of Proposition 3: Consider the function $V_0 := 1 - \boldsymbol{k}\cdot\boldsymbol{k}_r$, which is non-negative and vanishes only when $\boldsymbol{k} = \boldsymbol{k}_r$ since $|\boldsymbol{k}| = |\boldsymbol{k}_r| = 1$. Recall that $\boldsymbol{\omega}_r = \boldsymbol{k}_r \times \dot{\boldsymbol{k}}_r$. From (19), $\dot{\boldsymbol{k}}_r = \boldsymbol{\omega}_r \times \boldsymbol{k}_r$ so that

$$\begin{aligned} \dot{V}_0 &= -\dot{\boldsymbol{k}}\cdot\boldsymbol{k}_r - \boldsymbol{k}\cdot\dot{\boldsymbol{k}}_r \\ &= -(\boldsymbol{\omega}\times\boldsymbol{k})\cdot\boldsymbol{k}_r - \boldsymbol{k}\cdot(\boldsymbol{\omega}_r\times\boldsymbol{k}_r) \\ &= (\boldsymbol{\omega}_r - \boldsymbol{\omega})\cdot(\boldsymbol{k}\times\boldsymbol{k}_r) \end{aligned} \tag{20}$$

where the last equality follows from (19). Now, define

$$\begin{aligned} V_1 &:= \frac{\gamma^2(t)}{2}\frac{1-\boldsymbol{k}\cdot\boldsymbol{k}_r}{1+\boldsymbol{k}\cdot\boldsymbol{k}_r} \\ &= \frac{\gamma^2(t)}{2}\frac{1-(\boldsymbol{k}\cdot\boldsymbol{k}_r)^2}{(1+\boldsymbol{k}\cdot\boldsymbol{k}_r)^2} = \frac{\gamma^2(t)}{2}\frac{|\boldsymbol{k}\times\boldsymbol{k}_r|^2}{(1+\boldsymbol{k}\cdot\boldsymbol{k}_r)^2} \end{aligned} \tag{21}$$

where the last equality comes from that $(\boldsymbol{k}\cdot\boldsymbol{k}_r)^2 + |\boldsymbol{k}\times\boldsymbol{k}_r|^2 = 1$, since $|\boldsymbol{k}| = |\boldsymbol{k}_r| = 1$. One verifies that

$$\dot{V}_1 = \gamma(t)\dot{\gamma}(t)\frac{1-\boldsymbol{k}\cdot\boldsymbol{k}_r}{1+\boldsymbol{k}\cdot\boldsymbol{k}_r} + \gamma^2(t)\frac{\dot{V}_0}{(1+\boldsymbol{k}\cdot\boldsymbol{k}_r)^2}$$

and it follows from (20) and (21) that

$$\begin{aligned} \dot{V}_1 &= \gamma(t)\dot{\gamma}(t)\frac{|\boldsymbol{k}\times\boldsymbol{k}_r|^2}{(1+\boldsymbol{k}\cdot\boldsymbol{k}_r)^2} + \gamma^2(t)\frac{(\boldsymbol{k}\times\boldsymbol{k}_r)\cdot(\boldsymbol{\omega}_r-\boldsymbol{\omega})}{(1+\boldsymbol{k}\cdot\boldsymbol{k}_r)^2} \\ &= \gamma(t)\frac{\boldsymbol{k}\times\boldsymbol{k}_r}{(1+\boldsymbol{k}\cdot\boldsymbol{k}_r)^2}\big(\dot{\gamma}(t)\,\boldsymbol{k}\times\boldsymbol{k}_r + \gamma(t)(\boldsymbol{\omega}_r-\boldsymbol{\omega})\big) \end{aligned}$$

Replacing $\boldsymbol{\omega}$ by its expression (11) yields

$$\dot{V}_1 = -k_1(\boldsymbol{k},t)\gamma^2(t)\frac{|\boldsymbol{k}\times\boldsymbol{k}_r|^2}{(1+\boldsymbol{k}\cdot\boldsymbol{k}_r)^2} = -2k_1(\boldsymbol{k},t)V_1 \tag{22}$$

Since $\inf_{\boldsymbol{k},t} k_1(\boldsymbol{k},t) > 0$, V_1 converges exponentially to zero. Exponential stability of $\boldsymbol{k} = \boldsymbol{k}_r$ then follows from the definition of V_1 and the fact that $\inf_t \gamma(t) > 0$.

Proof of Proposition 4: In view of Assumption 2, $\boldsymbol{k}_r$ is well defined in a neighborhood of the equilibrium point $(\tilde{\boldsymbol{\rho}}, \boldsymbol{v}, \boldsymbol{k}) = (\boldsymbol{0}, \boldsymbol{v}_r, \boldsymbol{k}_r)$. Note also that $\gamma(t) \geq \sqrt{c_2} > 0$. Therefore, the feedback law is well defined in a neighborhood of the equilibrium point. From (2) and (8), $\boldsymbol{F}_p - T_p\boldsymbol{k} = \boldsymbol{F}_a - T\boldsymbol{k}$. Therefore $\bar{\boldsymbol{F}}_p - T_p\boldsymbol{k} = \bar{\boldsymbol{F}}_a - T\boldsymbol{k}$ and $\bar{\boldsymbol{F}}_p \cdot \boldsymbol{k} = T_p - T + \bar{\boldsymbol{F}}_a \cdot k = T_p$. From this relation and (14), Eq. (12) can be written as:

$$\begin{aligned} m\dot{\tilde{\boldsymbol{v}}} &= |\bar{\boldsymbol{F}}_p|\boldsymbol{k}_r - T_p\boldsymbol{k} + m\boldsymbol{\xi}(\tilde{\boldsymbol{\rho}}, \tilde{\boldsymbol{v}}) \\ &= |\bar{\boldsymbol{F}}_p|\boldsymbol{k}_r - (\bar{\boldsymbol{F}}_p \cdot \boldsymbol{k})\boldsymbol{k} + m\boldsymbol{\xi}(\tilde{\boldsymbol{\rho}}, \tilde{\boldsymbol{v}}) \\ &= |\bar{\boldsymbol{F}}_p|\boldsymbol{k}_r - (|\bar{\boldsymbol{F}}_p|\boldsymbol{k}_r \cdot \boldsymbol{k})\boldsymbol{k} + m\boldsymbol{\xi}(\tilde{\boldsymbol{\rho}}, \tilde{\boldsymbol{v}}) \\ &= |\bar{\boldsymbol{F}}_p|(\boldsymbol{k}_r - (\boldsymbol{k}_r \cdot \boldsymbol{k})\boldsymbol{k}) + m\boldsymbol{\xi}(\tilde{\boldsymbol{\rho}}, \tilde{\boldsymbol{v}}) \\ &= |\bar{\boldsymbol{F}}_p|(\boldsymbol{k} \times (\boldsymbol{k}_r \times \boldsymbol{k})) + m\boldsymbol{\xi}(\tilde{\boldsymbol{\rho}}, \tilde{\boldsymbol{v}}) \end{aligned} \tag{23}$$

where the last equality comes from (19). Therefore, along the solutions to the controlled system, the variables $\tilde{\boldsymbol{\rho}}$ and $\tilde{\boldsymbol{v}}$ satisfy Eq. (17) with $\varepsilon := \frac{1}{m}|\bar{\boldsymbol{F}}_p|(\boldsymbol{k} \times (\boldsymbol{k}_r \times \boldsymbol{k}))$. Since $\boldsymbol{k}$ and $\boldsymbol{k}_r$ are unit vectors, it follows from (21) and the definition of γ that

$$\begin{aligned} V_1 &\geq \frac{\gamma^2(t)}{8}|\boldsymbol{k} \times \boldsymbol{k}_r|^2 \geq \frac{|\bar{\boldsymbol{F}}_p|^2}{8}|\boldsymbol{k} \times \boldsymbol{k}_r|^2 \\ &\geq \frac{|\bar{\boldsymbol{F}}_p|^2}{8}|\boldsymbol{k} \times (\boldsymbol{k} \times \boldsymbol{k}_r)|^2 \geq \frac{m^2|\varepsilon|^2}{8} \end{aligned} \tag{24}$$

From the proof of Proposition 3, V_1 converges to zero exponentially so that ε also converges to zero exponentially. From Assumption 1 and converse Lyapunov theorems (See, e.g., [25, Section 4.7]) there exists a quadratic Lyapunov function $V_2(\tilde{\boldsymbol{\rho}}, \tilde{\boldsymbol{v}})$ for System (16), i.e., such that in a neighborhood of $(\tilde{\boldsymbol{\rho}}, \tilde{\boldsymbol{v}}) = (\boldsymbol{0}, \boldsymbol{0})$,

$$\dot{V}_2(\tilde{\boldsymbol{\rho}}, \tilde{\boldsymbol{v}}) \leq -k_2 V_2(\tilde{\boldsymbol{\rho}}, \tilde{\boldsymbol{v}}) \tag{25}$$

Using the triangular inequality, it follows from (22), (17), (24), and (25) that $V = \alpha V_1 + V_2$ is a Lyapunov function for the controlled system for $\alpha > 0$ large enough.

References

[1] S. N. Singh, A. Schy, Output feedback nonlinear decoupled control synthesis and observer design for maneuvering aircraft, Int. Journal of Control 31 (1980) 781–806.

[2] Q. Wang, R. Stengel, Robust nonlinear flight control of high-performance aircraft, IEEE Transactions on Control Systems Technology 13 (1) (2005) 15–26.

[3] E. Muir, Robust flight control design challenge problem formulation and manual: The high incidence research model (hirm), in: Robust Flight Control, A Design Challenge (GARTEUR), Vol. 224 of Lecture Notes in Control and Information Sciences, Springer Verlag, 1997, pp. 419–443.

[4] J. Hauser, S. Sastry, G. Meyer, Nonlinear control design for slightly non-minimum phase systems: Application to V/STOL, Automatica 28 (1992) 651–670.

[5] A. Isidori, L. Marconi, A. Serrani, Robust autonomous guidance: an internal-model based approach., Springer Verlag, 2003.

[6] S. Bouabdallah, R. Siegwart, Backstepping and sliding-mode techniques applied to an indoor micro quadrotor, in: IEEE International Conference on Robotics and Automation, 2005.

[7] R. Xu, U. Ozguner, Sliding mode control of a class of underactuated systems, Automatica 44 (2008) 233–241.

[8] H. J. Kim, D. H. Shim, S. Sastry, Nonlinear model predictive tracking control for rotorcraft-based unmanned aerial vehicles, in: ACC, 2002, pp. 3576–3581.

[9] M.-D. Hua, T. Hamel, P. Morin, C. Samson, Introduction to feedback control of underactuated vtol vehicles, IEEE Control Systems Magazine (2013) 61–75.

[10] N. Guenard, T. Hamel, V. Moreau, Dynamic modeling and intuitive control strategy for an "x4-flyer", in: Int. Conf. on Control and Automation, 2005, pp. 141–146.

[11] M.-D. Hua, T. Hamel, P. Morin, C. Samson, A control approach for thrust-propelled underactuated vehicles and its application to VTOL drones, IEEE Trans. on Automatic Control 54(8) (2009) 1837–1853.

[12] D. Pucci, Towards a unified approach for the control of aerial vehicles, Ph.D. thesis, Université de Nice-Sophia Antipolis and "Sapienza" Universita di Roma (2013).

[13] P. Pounds, R. Mahony, P. Corke, Modelling and control of a large quadrotor robot, Control Engineering Practice (2010) 691–699.

[14] P. Bristeau, P. Martin, E. Salaun, The role of propeller aerodynamics in the model of a quadrotor UAV, in: European Control Conference, 2009, pp. 683–688.

[15] J.-M. Pflimlin, Commande d'un minidrone à hélice carénée: de la stabilisation dans le vent à la navigation autonome (in french), Ph.D. thesis, Toulouse University (2006).

[16] J. Anderson, Fundamentals of Aerodynamics, McGraw Hill Series in Aeronautical and Aerospace Engineering, 2010.

[17] R. F. Stengel, Flight Dynamics, Princeton Uni. Press, 2004.

[18] H. Huang, G. M. Hoffmann, S. L. Waslander, C. J. Tomlin, Aerodynamics and Control of Autonomous Quadrotor Helicopters in Aggressive Maneuvering, in: IEEE Conf. on Robotics and Automation, 2009, pp. 3277–3282.

[19] E. N. Johnson, M. A. Turbe, Modeling, control, and flight testing of a small ducted fan aircraft, Journal of Guidance, Control, and Dynamics 29(4) (2006) 769–779.

[20] R. Naldi, Prototyping, modeling and control of a class of VTOL aerial robots, Ph.D. thesis, Bologna University (2008).

[21] R. Prouty, Helicopter Performance, Stability, and Control, Krieger, 2005.

[22] J. W. Keyes, Aerodynamic characteristics of lenticular and elliptic shaped configurations at a mach number of 6, Tech. Rep. NASA-TN-D-2606, NASA (1965).

[23] B. F. Saffel, M. L. Howard, E. N. Brooks, A method for predicting the static aerodynamic characteristics of typical missile configurations for angles of attack to 180 degrees., Tech. Rep. AD0729009, Department of the navy naval ship research and development center (1971).

[24] M.-D. Hua, C. Samson, Time sub-optimal nonlinear pi and pid controllers applied to longitudinal headway car control, Int. Journal of Control 84-10 (2011) 1717–1728.

[25] H. Khalil, Nonlinear systems, Prentice Hall, 2002.